Cao et al. *Zool. Res.* 2021, 42(5): 562−573
https://doi.org/10.24272/j.issn.2095-8137.2021.075

ZR | Zoological Research

Article Open Access

Chromatin remodeler INO80 mediates trophectoderm permeability barrier to modulate morula-to-blastocyst transition

Zu-Bing Cao[1,#], Di Gao[1,#], Hui-Qun Yin[2,#], Hui Li[1,#], Teng-Teng Xu[1], Meng-Ya Zhang[1], Xin Wang[1], Qiu-Chen Liu[1], Ye-Lian Yan[1], Yang-Yang Ma[1], Tong Yu[1], Yun-Sheng Li[1], Yun-Hai Zhang[1,*]

[1] *Anhui Province Key Laboratory of Local Livestock and Poultry*, *Genetical Resource Conservation and Breeding*, *College of Animal Science and Technology*, *Anhui Agricultural University*, *Hefei*, *Anhui* 230036, *China*
[2] *Reproductive Medicine Center*, 901*st Hospital*, *Hefei*, *Anhui* 230031, *China*

ABSTRACT

Inositol requiring mutant 80 (INO80) is a chromatin remodeler that regulates pluripotency maintenance of embryonic stem cells and reprogramming of somatic cells into pluripotent stem cells. However, the roles and mechanisms of INO80 in porcine pre-implantation embryonic development remain largely unknown. Here, we show that INO80 modulates trophectoderm epithelium permeability to promote porcine blastocyst development. The INO80 protein is highly expressed in the nuclei during morula-to-blastocyst transition. Functional studies revealed that RNA interference (RNAi)-mediated knockdown of *INO80* severely blocks blastocyst formation and disrupts lineage allocation between the inner cell mass and trophectoderm. Mechanistically, single-embryo RNA sequencing revealed that INO80 regulates multiple genes, which are important for lineage specification, tight junction assembly, and fluid accumulation. Consistent with the altered expression of key genes required for tight junction assembly, a permeability assay showed that paracellular sealing is defective in the trophectoderm epithelium of *INO80* knockdown blastocysts. Importantly, aggregation of 8-cell embryos from the control and *INO80* knockdown groups restores blastocyst development and lineage allocation via direct complementation of the defective trophectoderm epithelium. Taken together, these results demonstrate that INO80 promotes blastocyst development by regulating the expression of key genes required for lineage specification, tight junction assembly, and fluid accumulation.

Keywords: INO80; Blastocyst; Trophectoderm; Tight junction; Permeability

INTRODUCTION

Fertilized embryos undergo several cell divisions to give rise to blastocysts. Concomitant with blastocyst formation, the trophectoderm (TE) and inner cell mass (ICM) lineages are generated (Chazaud & Yamanaka, 2016; White & Plachta, 2020). The establishment of a functional TE epithelium is

Received: 15 June 2021; Accepted: 30 July 2021; Online: 02 August 2021
Foundation items: This work was supported by the Anhui Provincial Natural Science Foundation (1908085MC97, 2008085MC85), National Natural Science Foundation of China (31802059, 31902226), Hefei Innovation and Entrepreneurship Support Plan for Returnee Scholar (03082009), and Anhui Provincial Innovation and Entrepreneurship Support Plan for Returnee Scholar (2020LCX015)
[#]Authors contributed equally to this work
*Corresponding author, E-mail: yunhaizhang@ahau.edu.cn

essential for blastocyst formation. The permeability of the TE to small molecules and water strictly regulates blastocoel formation and expansion (Cockburn & Rossant, 2010). These permeability features are mainly mediated by the action of tight junction (TJ) complexes, ion gradient pumps, H_2O channels, and cell polarity proteins (Cockburn & Rossant, 2010; Marikawa & Alarcon, 2012). Correct expression of the proteins assembled on the TE apical and basolateral membrane is required for blastocyst development (Alarcon, 2010; Marikawa & Alarcon, 2012; Wang et al., 2008). However, the adenosine triphosphate (ATP)-dependent chromatin remodelers responsible for regulating TE development remain largely unknown.

Numerous studies have revealed the critical role of ATP-dependent chromatin remodeling in the regulation of gene expression during pre-implantation embryonic development (Cabot & Cabot, 2018; Hota & Bruneau, 2016; Paul & Knott, 2014). The INO80 protein is a core ATPase component of the INO80 chromatin-remodeling complex, which contains four isotypes, i.e., *INO80B*, *INO80C*, *INO80D*, and *INO80E*. INO80 has been implicated in diverse nuclear processes, including DNA replication (Poli et al., 2017), DNA repair (Morrison, 2017), heterochromatin inheritance (Shan et al., 2020), and transcription regulation (Hota & Bruneau, 2016). In the cellular context, INO80 is reported to be involved in regulating differentiation and pluripotency maintenance of embryonic stem cells (Qiu et al., 2016; Wang et al., 2014), reprogramming of somatic cells into pluripotent stem cells (Wang et al., 2014), and spermatogenesis (Serber et al., 2016). In mice, embryos with loss of zygotic *INO80* arrest at the post-implantation stage and ICM cells derived from *INO80*-deleted blastocysts cease proliferation during outgrowth culture (Lee et al., 2014). In addition, depletion of maternal and zygotic *INO80* not only causes failure of blastocyst formation, but also alters the expression of pluripotency genes (Wang et al., 2014). These previous studies indicated that INO80 is essential for the specification of pluripotent ICM lineages during early embryogenesis in mice. However, recent study showed that INO80 is simultaneously localized in the nuclei of ICM and TE cells in mouse blastocysts (Wang et al., 2014). Thus, we speculate that INO80 may play a much broader role in blastocyst formation, beyond its established role in regulating ICM lineage specification.

Pigs are increasingly used as a translational model for human reproduction due to their similarity to human anatomy, physiology, developmental timing, and genetics (Alberio, 2020; Mordhorst & Prather, 2017; Prather et al., 2013). In the present study, we examined the function and regulatory mechanisms of INO80 during early porcine embryonic development. We found that INO80 mRNA and protein are widely expressed in early porcine embryos. Functional studies using RNAi showed that INO80 is essential for porcine blastocyst development. Using single-embryo transcriptomic analyses and chimeric embryos, we demonstrated that INO80 regulates the expression of multiple genes required for lineage specification, TJ assembly, and fluid accumulation, and its knockdown impairs TE barrier function in blastocyst development. Our findings provide new insights into the regulatory mechanisms of chromatin remodeling in porcine blastocyst development.

MATERIALS AND METHODS

Ethics statement

All experiments were conducted in accordance with the Institutional Animal Care and Use Committee (IACUC) guidelines under current approved protocols at Anhui Agricultural University (Approval No. SYXK2016-007).

Oocyte maturation

Ovaries were collected from a local slaughterhouse. Follicular fluid was aspirated from antral follicles 3–6 mm in diameter. Cumulus-oocyte complexes (COCs) were selected under a stereomicroscope. The COCs were then cultured in one well of a 4-well plate containing 400 μL of *in vitro* maturation medium (TCM-199 supplemented with 5% fetal bovine serum (FBS), 10% porcine follicular fluid, 10 IU/mL equine chorionic gonadotrophin (eCG), 5 IU/mL human chorionic gonadotropin (hCG), 100 ng/mL L-cysteine, 10 ng/mL epidermal growth factor (EGF), 0.23 ng/mL melatonin, 2.03×10^{-5} ng/mL leukemia inhibitory factor (LIF), 2×10^{-5} ng/mL insulin growth factor 1 (IGF-1), 4×10^{-5} ng/mL fibroblast growth factor 2 (FGF-2), 100 U/mL penicillin, and 100 mg/mL streptomycin) for 44 h at 38.5 °C, 5% CO_2, and saturated humidity. The cumulus cells surrounding the oocytes were removed using 1 mg/mL hyaluronidase following maturation.

Parthenogenetic activation (PA)

Mature oocytes were stimulated using two direct current pulses (1.56 kV/cm for 80 ms) in activation medium. The activated oocytes were then washed three times in porcine zygote medium (PZM-3) and incubated in chemically assisted activation medium at 38.5 °C for 4 h. The embryos were subsequently cultured in PZM-3 droplets at 38.5 °C, 5% CO_2, and 95% air with saturated humidity.

In vitro fertilization (IVF)

Metaphase II oocytes were washed in modified Tris-buffered medium (mTBM) containing 2 mg/mL bovine serum albumin (BSA) and 2 mmol/L caffeine. Approximately 15 oocytes were incubated in 50 μL of mTBM droplets for 4 h at 38.5 °C and 5% CO_2 in air. Semen from two boars was mixed and centrifuged at 1 900 *g* for 4 min at 38.5 °C in Dulbecco's phosphate-buffered saline (DPBS) supplemented with 1 mg/mL BSA (pH 7.3). The sperm were then resuspended with mTBM to a concentration of 1×10^6 cells/mL. The sperm solution (50 μL) was added to the mTBM droplets containing oocytes. After co-incubation of the oocytes and sperm at 38.5 °C for 6 h, the sperm surrounding the oocytes were washed out and the presumptive zygotes were cultured in PZM-3 at 38.5 °C and 5% CO_2 in air.

Real-time quantitative polymerase chain reaction (qPCR)

Total RNA was extracted from the oocytes and embryos using a RNeasy Mini Kit (Qiagen, 74104, Germany). RNA was transcriptionally reversed into cDNA using a QuantiTect Reverse Transcription Kit (Qiagen, 205311, Germany). The primers used in this study are listed in Supplementary Table S1. The PCR assembly was prepared in FastStart SYBR

Green Master mix (Roche, 04673514001, Germany) and run on a StepOne Plus™ Real-Time PCR System (Applied Biosystems, USA). Samples were collected three times and three biological replicates were conducted for each gene. *EF1A1* was used as the internal reference gene. The quantification cycle (Cq) values were obtained and analyzed using the $2^{-\Delta\Delta Ct}$ method.

Immunofluorescence staining

Oocytes and embryos were fixed in 4% paraformaldehyde solution for 15 min, permeabilized with 1% Triton X-100 for 30 min at room temperature (RT), and then blocked with 2% BSA at RT for 1 h. Samples were incubated in solution containing primary antibodies overnight at 4 °C. After washing, the samples were incubated for 1 h in solution containing secondary antibodies in the dark at 37 °C. Following washing, samples were counterstained with 4,6-diamidino-2-phenylindole dihydrochloride or propidium iodide for 10 min and were then loaded onto glass slides. Samples were then imaged using laser scanning confocal microscopy (Olympus, Japan). Information regarding primary and secondary antibodies is provided in Supplementary Tables S2, S3.

Microinjection

The small interfering RNA (siRNA) species was designed to target three different sites of the porcine *INO80* coding region (GenePharma, China). Information on the siRNA sequences used in this study is listed in Supplementary Table S4. Microinjection was performed in T2 (TCM199 with 2% FBS) medium containing 7.5 μg/mL cytochalasin B on an inverted microscope (Olympus, Japan). Approximately 10 pL of siRNA solution (50 μmol/L) was microinjected into the cytoplasm of MII oocytes. Embryos were cultured in PZM-3 medium for 7 days.

Western blotting

A total of 50 embryos were collected in 10 μL of lysis buffer (RIPA buffer supplemented with a cocktail of protease inhibitors) and stored at –80 °C. Samples were then mixed with protein sample buffer (Beyotime, China) and heated at 95 °C for 5 min. Proteins were separated using a sodium dodecyl sulfate polyacrylamide gel electrophoresis (SDS-PAGE) system (Tanon, China) at 100 V for 120–150 min. The proteins were transferred to polyvinylidene fluoride (PVDF) membranes with an electrophoretic transfer apparatus (Tanon, China) at 65 V for 120 min. Thereafter, membranes were blocked in blocking buffer (Beyotime, China) for 2 h and then incubated with primary antibodies at 4 °C overnight. After washing, the membranes were incubated with secondary antibodies at RT for 1.5–2 h. Signals were detected with a Lumi-Light Western Blotting Substrate (Roche, Germany) and images were acquired using a VersaDoc Imaging System (Bio-Rad, USA). The signal intensity of bands was measured as integrated intensity with Image J and normalized to background intensity. Details on primary and secondary antibodies used in this study are provided in Supplementary Tables S2, S3.

Single-embryo RNA sequencing (RNA-seq)

Single blastocysts at day 5 (non-injected, control-siRNA injected, and *INO80*-siRNA injected embryos) were collected for RNA-seq analysis. RNA was extracted using a RNeasy Mini Kit (Qiagen, 74104, Germany). Pre-amplified cDNA was fragmented using fragmentase (NEB, M0348S, England) via incubation at 37 °C for 20 min. The cDNA libraries were constructed using a TruSeq Nano DNA LT Library Preparation Kit (Illumina, FC-121-4001, USA). The libraries were then sequenced using the Illumina HiSeq 2500 platform (LC-Sciences, China). Reads were mapped to the pig reference genome. Differential gene expression between non-injected, control siRNA-injected, and *INO80* siRNA-injected embryos was determined using Cufflinks (v2.2). The threshold for significance was a false discovery rate ≤0.05 and an expression fold-change ≥2. Gene Ontology (GO) analysis was performed using DAVID Bioinformatics Resources v6.8. RNA-seq data are presented in Supplementary Tables S5, S6.

Trophectoderm permeability by fluorescein isothiocyanate (FITC)-dextran exclusion test

Blastocysts were incubated in modified PZM-3 medium containing 1 mg/mL 40 kDa FITC-dextran (Sigma, FD40, USA) at 38.5 °C for 40 min. The blastocysts were then immediately washed and visualized under an inverted fluorescence microscope. Blastocysts showing green fluorescence were defined as having impaired permeability.

Generation of chimeras by aggregation

Zona pellucidae of 8-cell embryos from the uninjected and *INO80* siRNA-injected groups were removed by pronase. Following washing with PZM-3, two zona pellucida-free embryos were paired in microwells to produce chimeric embryos. Chimeric embryos were cultured with PZM-3 at 38.5 °C for 168 h to observe blastocyst development.

Statistical analysis

Statistical analyses were performed using one-way analysis of variance (ANOVA) or student's *t*-test (SPSS 17.0). All experiments were carried out at least three times and were presented as mean±standard error of the mean (*SEM*). $P<0.05$ was considered statistically significant.

RESULTS

Developmental expression of INO80 mRNA and protein in early embryos

We performed qPCR to analyze *INO80* mRNA expression. Results showed that *INO80* mRNA was present in the oocytes and embryos, but its expression level was higher at the 1-cell, 2-cell, and 8-cell stages compared to the blastocyst stage (Figure 1A) ($P<0.05$). Further analysis of published mouse embryo microarray data (Zeng et al., 2004) revealed that the expression level of *INO80* mRNA was significantly higher at the 2-cell and 8-cell stages compared to the other developmental stages (Figure 1B) ($P<0.05$). Next, immunofluorescence staining was performed to determine the changes in and localization of INO80 protein expression in early embryos. INO80 antibody specificity in porcine embryos was verified prior to immunostaining (Supplementary Figure S1A). Results revealed that the INO80 protein was localized in

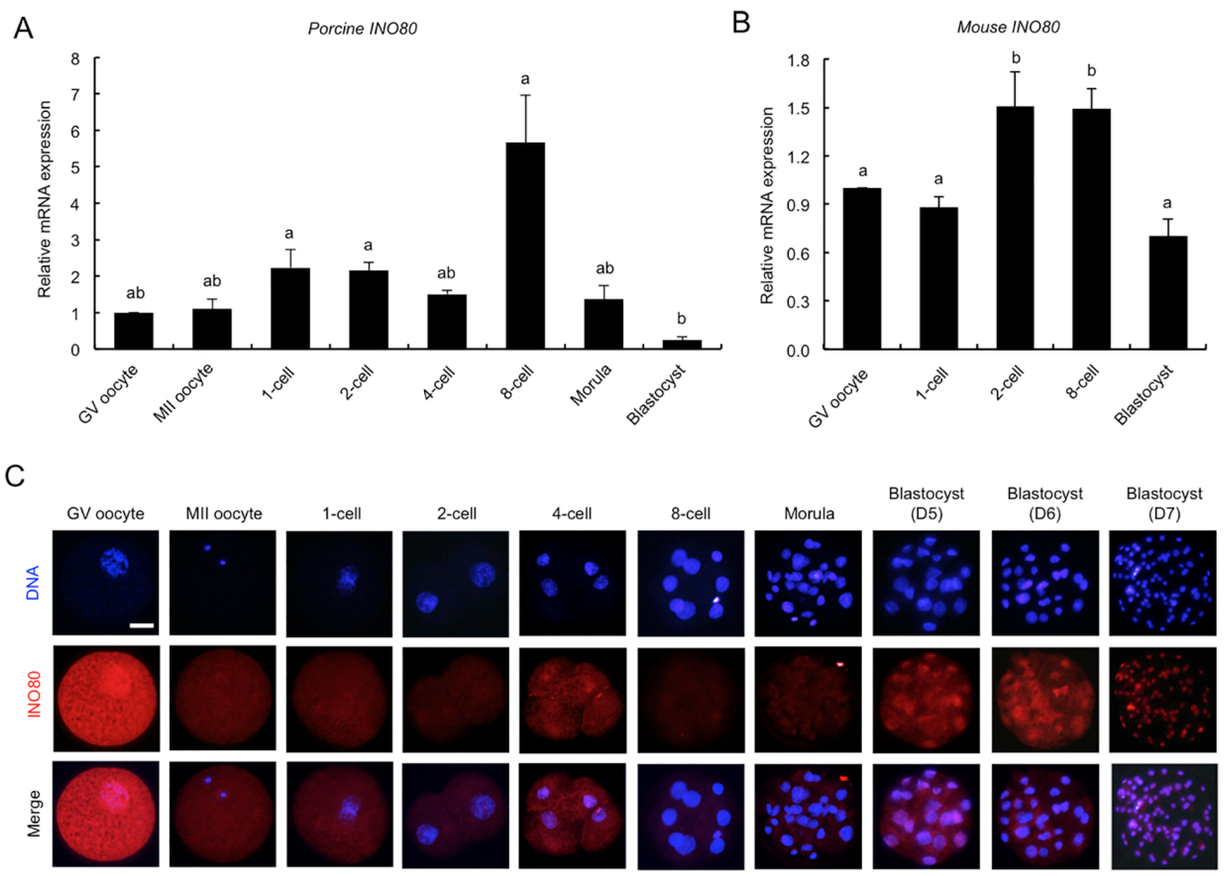

Figure 1 Expression of INO80 mRNA and protein in early porcine embryos

A: Expression of *INO80* mRNA in porcine oocytes and early embryos. Relative expression of *INO80* mRNA was determined by qPCR. Data were normalized against endogenous reference gene (*EF1α1*) and data from GV oocytes were set to 1. GV, germinal vesicle; MII, metaphase II. B: Expression of *INO80* mRNA in mouse oocytes and early embryos. Microarray data on *INO80* expression in mouse oocytes and embryos were obtained and analyzed from the GEO online repository (accession number: GSE6669156). C: Localization and expression of INO80 protein in porcine oocytes and early embryos. Representative images obtained by confocal microscopy are shown. Experiments were independently repeated three times with at least 30 oocytes/embryos per stage. Scale bar: 50 μm. Data are mean±*SEM* and different letters on bars indicate significant differences (P<0.05).

the cytoplasm from the GV oocyte to morula stages but was present in blastocyst nuclei from days 5 to 7 (Figure 1C). Additionally, INO80 protein levels in GV oocytes and blastocysts were higher than levels in embryos from the 1-cell to morula stages (Figure 1C). Thus, these results indicate that INO80 mRNA and protein are expressed in early porcine embryos.

RNAi-mediated efficient knockdown of INO80 mRNA and protein in early embryos

To uncover the role of INO80 in early embryonic development, RNAi was used to deplete INO80 mRNA and protein. MII oocytes were microinjected with siRNA against *INO80* or negative control (NC) siRNA. Uninjected MII oocytes served as the control. MII oocytes in each group were then parthenogenetically activated and cultured to the blastocyst stage. A subset of embryos at the 8-cell, morula, and blastocyst stages were subject to qPCR to detect the relative expression of *INO80* mRNA. Results showed that siRNA injection significantly decreased the levels of *INO80* mRNA at the 8-cell (Figure 2A), morula (Figure 2B), and blastocyst stages (Figure 2C) compared to the control groups (P<0.05). No differences in expression were observed between the NC siRNA-injected and uninjected control groups (Figure 2A–C). To confirm the specificity of the siRNA targeting effects, the expression levels of genes encoding other subunits in INO80 complexes were further examined by qPCR. *INO80* siRNA did not affect the expression levels of the *INO80B*, *INO80C*, *INO80D*, and *INO80E* transcripts (Supplementary Figure S2). Next, immunofluorescence and western blot analyses were performed to examine the relative amount of INO80 protein in the blastocysts at day 5. As shown in Figure 2D, the fluorescence signal of the INO80 protein was largely decreased in the injected embryos compared to the control groups. Correspondingly, western blotting revealed that *INO80* siRNA significantly reduced the INO80 protein levels (Figure 2E, F) (P<0.05). Collectively, these results demonstrate that *INO80* siRNA can efficiently knock down INO80 mRNA and protein in early embryos.

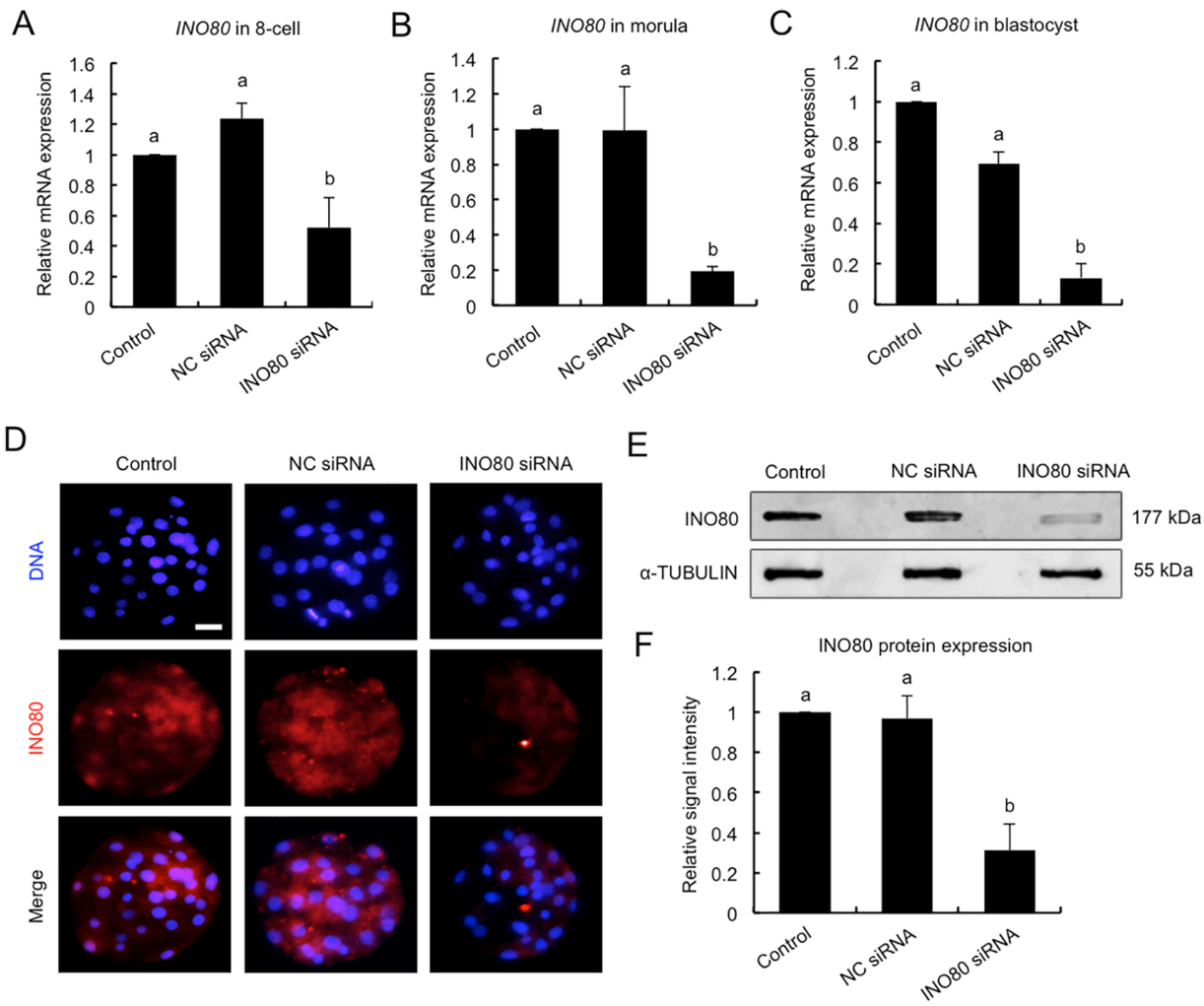

Figure 2 Verification of RNAi-mediated INO80 knockdown efficiency in early embryos

A–C: Relative abundance of *INO80* mRNA in 8-cell (A), morula (B), and blastocyst stages (C) in control, NC siRNA-injected, and *INO80* siRNA-injected groups was determined by qPCR. NC, negative control. D: Expression of INO80 protein in blastocysts. Embryos were stained for INO80 (red) and DNA (blue). Representative images obtained by confocal microscopy are shown. Experiments were independently repeated three times with at least 20 embryos per group. Scale bar: 50 μm. E: Western blot analysis of INO80 protein expression. Blastocysts were used for western blot analysis and α-tubulin was used as a loading control. Representative image is shown. F: Quantitative analysis of INO80 protein levels. Data are mean±*SEM* from three independent experiments and different letters on bars indicate significant differences (P<0.05).

INO80 knockdown impairs blastocyst development and disrupts normal lineage allocation

To ascertain whether *INO80* knockdown (KD) influences embryonic development, we compared the developmental rates of *INO80* KD embryos to NC siRNA-injected and uninjected embryos. Results showed that *INO80* KD did not affect developmental rates of PA embryos at the 2-cell, 4-cell, 8-cell, and morula stages (Supplementary Figure S3), but significantly reduced the blastocyst rates (days 5–7) compared to the control groups (Figure 3A, B) (P<0.05). Similarly, *INO80* KD had no effect on IVF embryonic development to the 2-cell, 4-cell, 8-cell, and morula stages (Supplementary Figure S4A), but caused a significant reduction in embryos that developed to the blastocyst stage (days 5–7) (Supplementary Figure S4B, C) (P<0.05). No differences in embryonic development were observed between the NC siRNA-injected and uninjected control groups (Figure 3A; Supplementary Figure S4B, C). Importantly, a small proportion of the *INO80* KD embryos developed to the blastocyst stage (Figure 3A), which allowed us to examine lineage allocation. Thus, blastocysts in each group were stained with a CDX2 antibody to determine the TE cell number (Figure 3C). The number of ICM cells was indirectly determined by subtracting the TE number from the total cell number. Results revealed that *INO80* KD led to a significant reduction in total, ICM, and TE cell number (Figure 3D) (P<0.05). In addition, the ratio of ICM cells to TE cells in the *INO80* KD blastocysts increased significantly compared to the control groups (Figure 3D) (P<0.05). These results demonstrate that INO80 is essential for blastocyst development and normal lineage allocation.

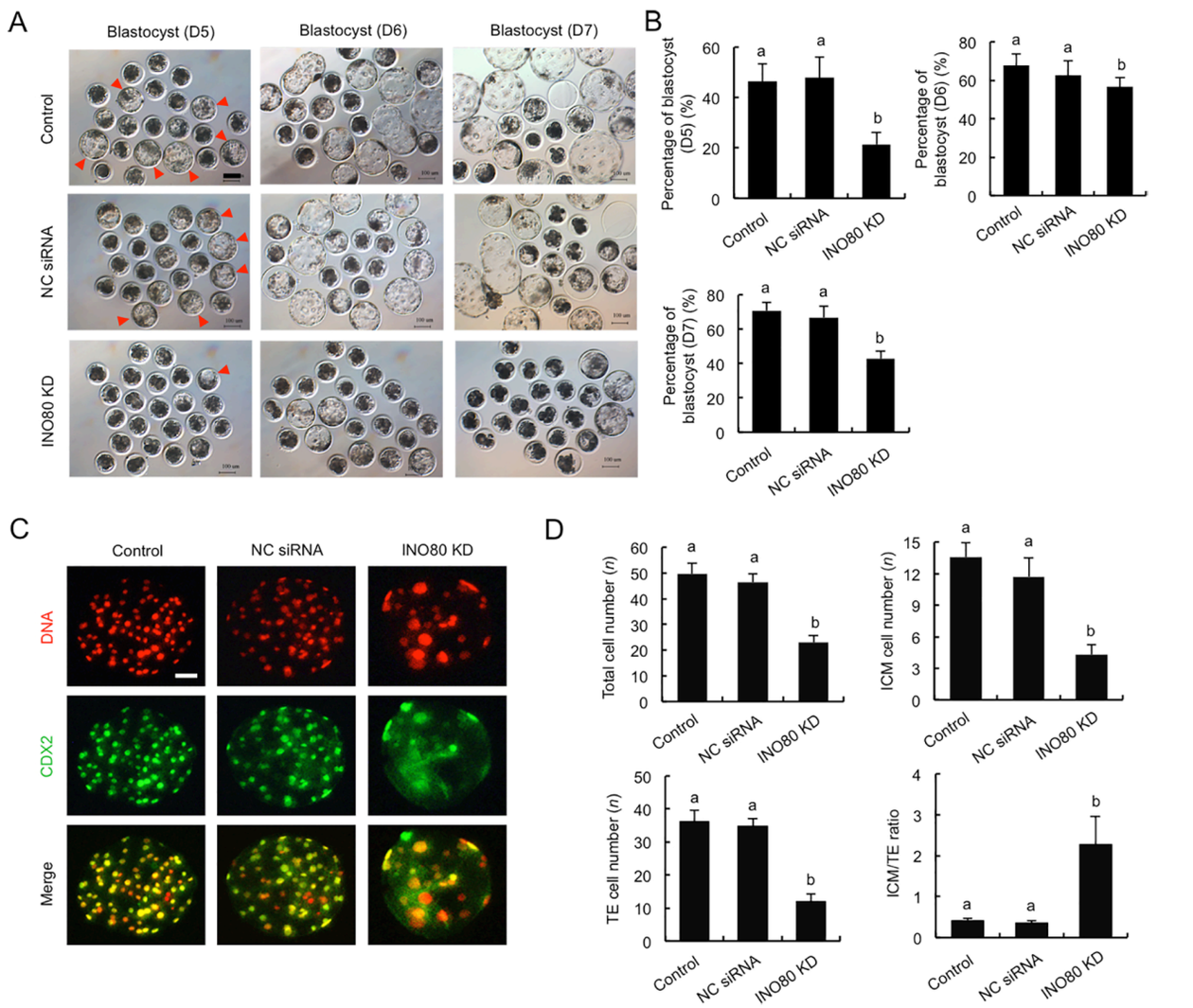

Figure 3 Effect of *INO80* knockdown on blastocyst development and lineage allocation

A: Representative images of blastocysts on days 5, 6, and 7. Scale bar: 100 μm. Red asterisks indicate blastocysts. B: Developmental rates of blastocysts on days 5, 6, and 7. C: Representative fluorescence images of blastocysts. Blastocysts were stained for CDX2 (green) and DNA (red). Experiments were independently repeated three times with at least 20 blastocysts per group. Scale bar: 50 μm. D: Lineage allocation analysis of *INO80* KD and control blastocysts. Total, ICM, and TE cell numbers and ICM to TE cell ratio were separately recorded and analyzed. ICM: inner cell mass; TE: trophectoderm. Data are mean±*SEM* and different letters on bars indicate significant differences (P<0.05).

INO80 knockdown perturbs early blastocyst transcriptome

To identify target genes regulated by INO80, single-embryo transcriptomic sequencing was performed in three groups of early blastocysts: i.e., *INO80* KD, NC siRNA-injected, and uninjected embryos. We identified 6417 differentially expressed genes (DEGs) between *INO80* KD and NC siRNA groups, and 3 020 DEGs between the *INO80* KD and control groups (Figure 4A). Among the DEGs, 1 051 were shared between the two sets (Figure 4A), including 350 down-regulated genes and 701 up-regulated genes (Figure 4B) (Supplementary Table S5). Next, we annotated the potential function of the shared DEGs using GO analyses. The DEGs were enriched in biological functions associated with epithelial characteristics, such as transmembrane transport, water transport, integral component of membrane, apical plasma membrane, and water channel activity (Figure 4C) (Supplementary Table S6). These data show that INO80 regulates the expression of multiple genes important for the differentiation of epithelial cells.

INO80 regulates expression of determinants required for ICM and trophectoderm lineage specification

Because *INO80* KD led to defects in both lineage allocation and expression of genes related to epithelial differentiation, we hypothesized that INO80 may regulate the expression of key genes important for ICM and TE lineage commitment. Thus, qPCR and immunofluorescence staining were performed on early blastocysts to determine the expression of lineage-specification genes, including *OCT4*, *SOX2*, *NANOG*, *CDX2*,

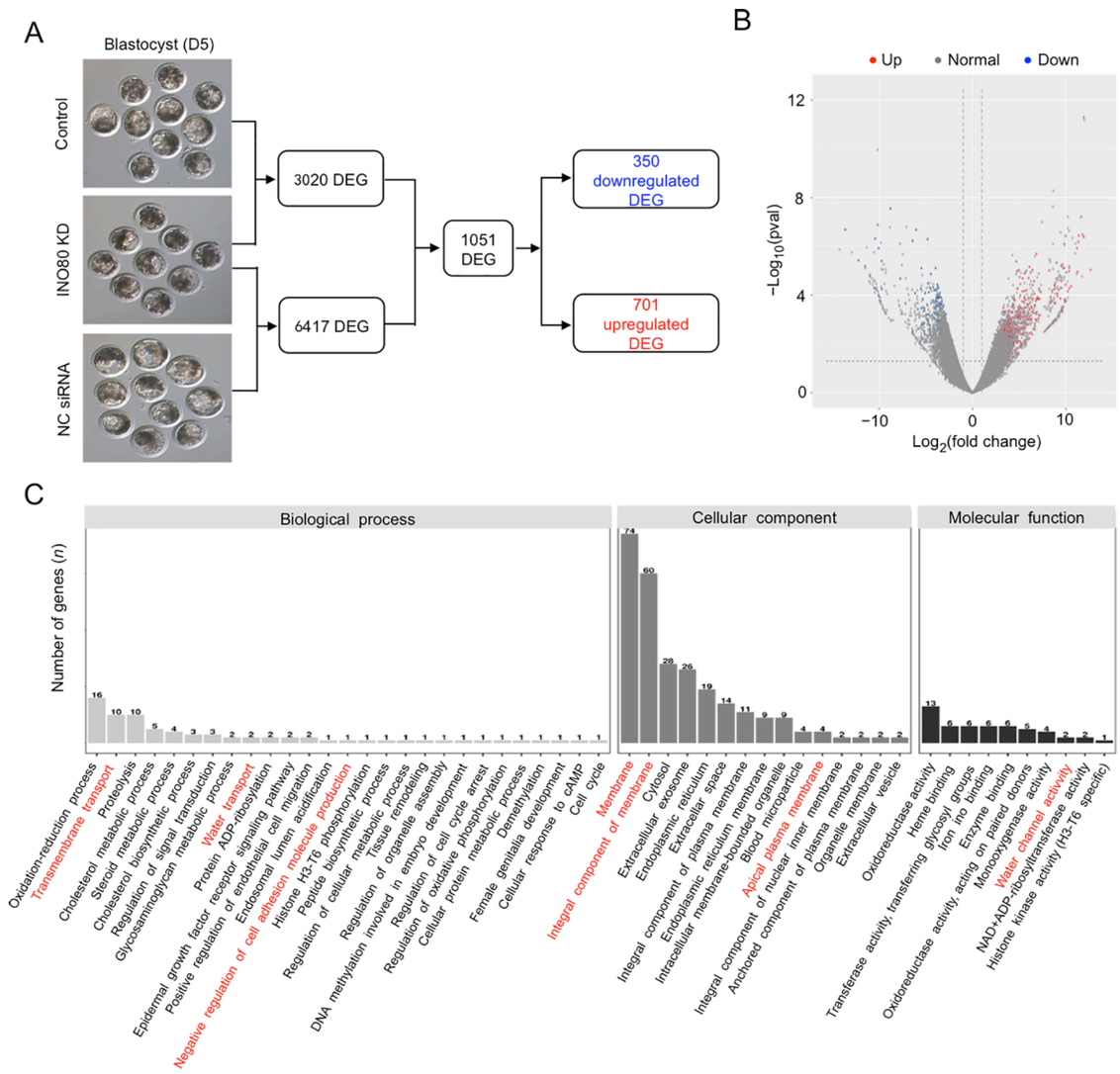

Figure 4 Effect of *INO80* knockdown on blastocyst transcriptome

A: Number of differentially expressed genes (DEGs) in blastocysts (Day 5) between control, NC siRNA, and *INO80* KD groups. Blue square denotes number of down-regulated genes; red square indicates number of up-regulated genes. B: Volcano plot of DEGs in blastocysts. Blue spots denote down-regulated genes; red spots indicate up-regulated genes. C: GO analyses show most enriched functional categories for DEGs after *INO80* KD. Red terms indicate functional categories associated with epithelial characteristics.

TEAD4, and *YAP*, which are important for blastocyst development in mice (Yagi et al., 2007), pigs (Bou et al., 2016; Cao et al., 2019; Emura et al., 2019), and cattle (Daigneault et al., 2018; Goissis & Cibelli, 2014; Negrón-Pérez & Hansen, 2018). The levels of *OCT4*, *CDX2*, and *TEAD4* mRNA were significantly reduced in the *INO80* KD blastocysts (Figure 5A, B) (P<0.05), whereas the expression levels of *SOX2* and *NANOG* mRNA were not affected in the blastocysts (Figure 5A). In addition, *YAP* expression was significantly increased in the *INO80* KD embryos (Figure 5B) (P<0.05). We further examined the expression and localization of OCT4 and YAP proteins, as the two genes were down-regulated and up-regulated by *INO80* KD, respectively. Consistent with the qPCR results, the OCT4 protein decreased dramatically in the *INO80* KD embryos compared to the controls (Figure 5C), whereas the YAP protein increased significantly in the *INO80* KD blastocysts (Figure 5D). These results indicate that INO80 is involved in regulating the expression of genes important for ICM and TE lineage specification.

INO80 modulates tight junction assembly and fluid accumulation to promote blastocyst development

To further unravel the molecular mechanisms underlying the developmental phenotypes of *INO80* KD embryos, we examined the expression of multiple genes required for TJ assembly and fluid accumulation. Results revealed that the expression levels of *ACTA2*, *ADAM19*, *ADAM21*, *OCLN*, and *CDH1* significantly decreased in *INO80* KD embryos (Figure 6A) (P<0.05). Likewise, the expression levels of cell polarity genes, such as *PRKCA*, *PRKCD*, *PRKCI*, *PRKCZ*, and *PHOA*, also significantly decreased (Figure 6A) (P<0.05). Furthermore, we observed a significant reduction in the

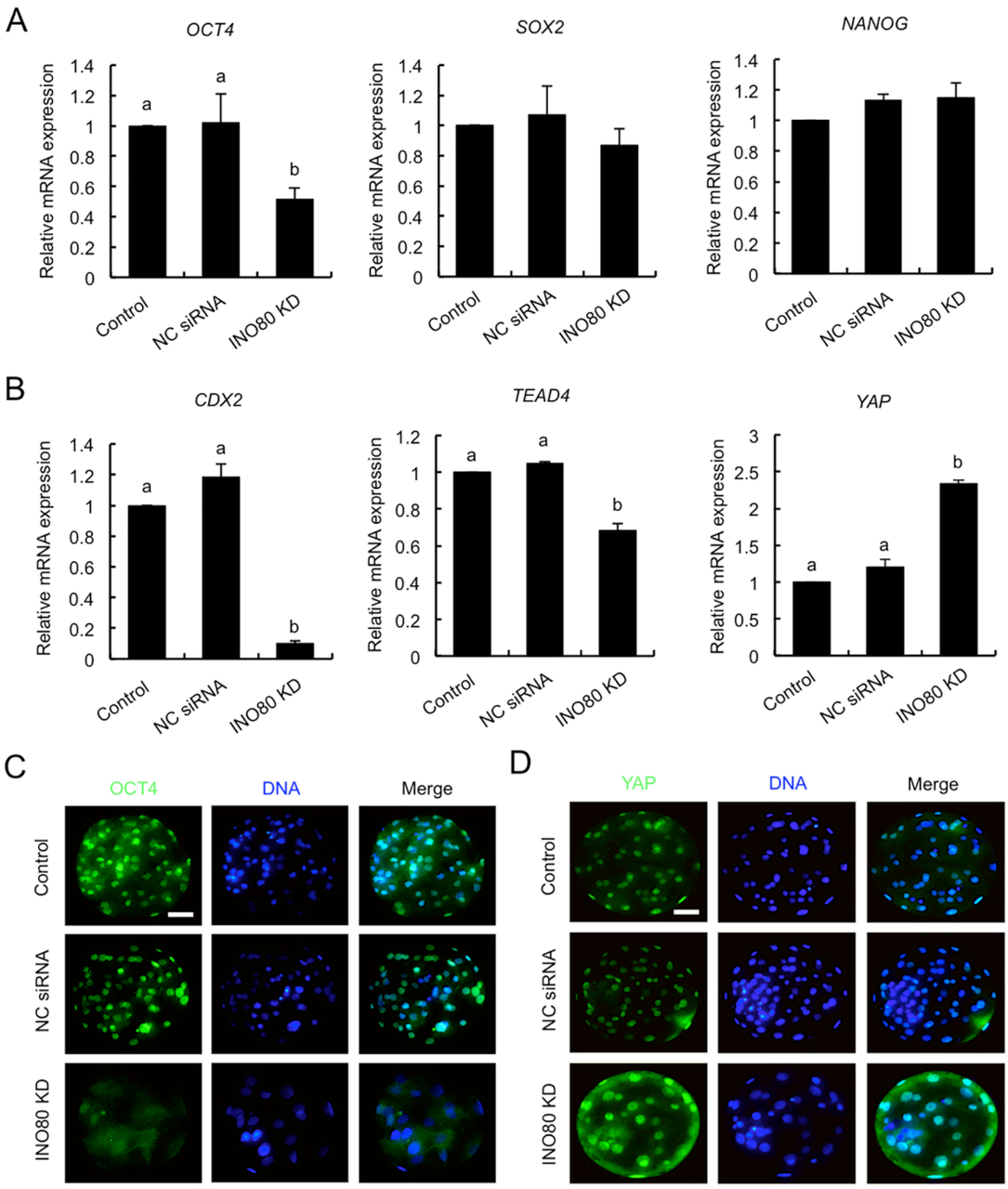

Figure 5 Effect of *INO80* knockdown on expression of genes important for ICM and TE lineage specification

A: Expression of pluripotency genes in blastocysts. Expression levels of *OCT4, SOX2*, and *NANOG* mRNA were determined by qPCR. B: Expression of genes required for TE specification in blastocysts. Relative abundance of *CDX2, TEAD4*, and *YAP* mRNA were determined by qPCR. All data were normalized against endogenous reference gene (*EF1α1*) and control group data were set to 1. Data are mean±*SEM* and different letters on bars indicate significant differences (P<0.05). Expression of OCT4 (C) and YAP (D) proteins by immunofluorescence. Blastocysts were stained for OCT4, CDX2 (green), and DNA (blue). Representative images are shown. Experiments were independently repeated three times with at least 20 blastocysts per group. Scale bar: 50 μm.

expression levels of fluid accumulation-related genes, including *ATP1A1*, *ATP1A3*, *AQP3*, *APQ9*, and *AQP11* in *INO80* KD embryos (Figure 6B) (P<0.05). We also examined the expression levels of cytoskeleton-related genes in embryos. Results showed that the expression levels of *FN1*, *KRT8*, *KRT23*, and ANXA7 were significantly reduced (Figure 6B) (P<0.05), whereas the expression of *SGK1* was not affected in the *INO80* KD embryos (Figure 6B). Consistent with the qPCR data, the apical and basolateral localized proteins, including OCLN and CDH1, were severely diminished in the *INO80* KD embryos compared to the controls (Figure 6C).

TJ complex-mediated paracellular sealing between TE cells is an essential prerequisite for blastocyst formation (Choi et

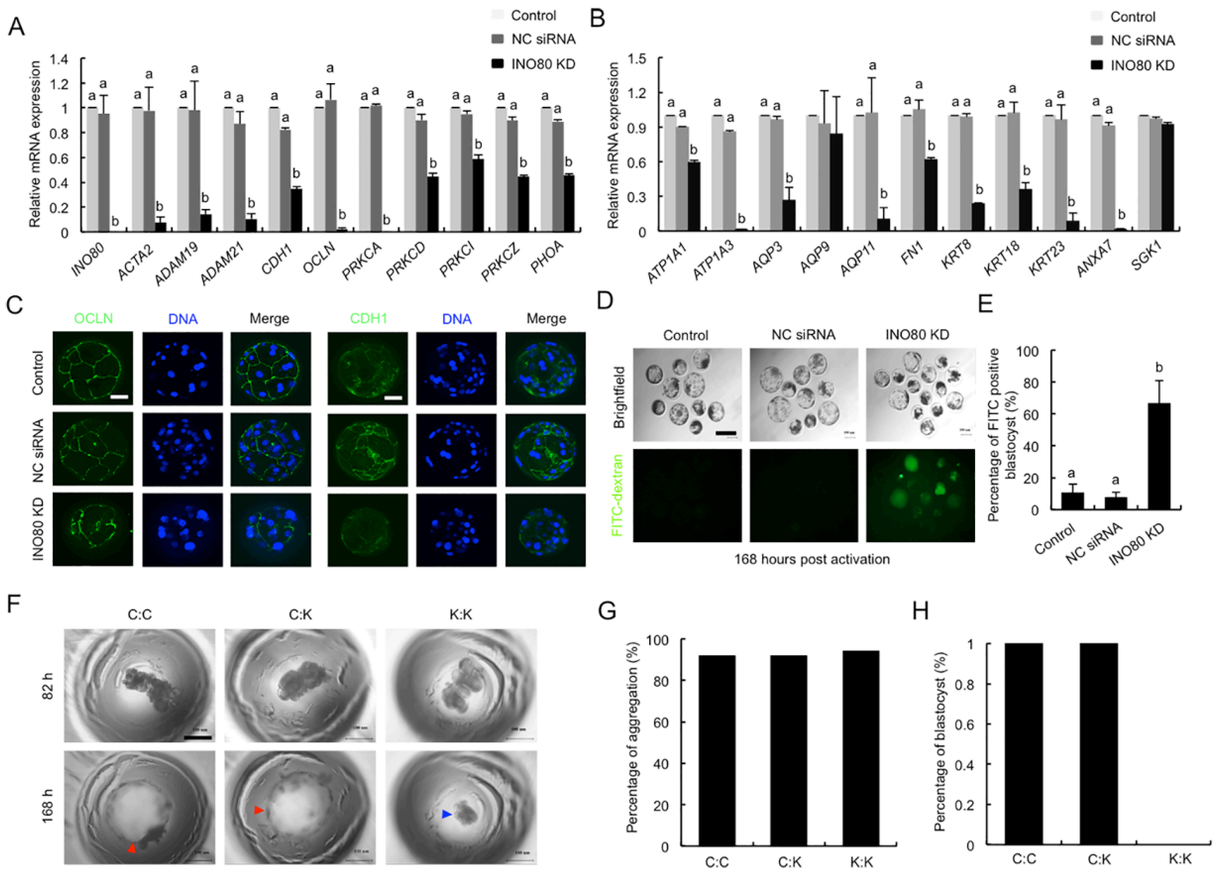

Figure 6 Effect of *INO80* knockdown on tight junction assembly and fluid accumulation

A, B: Expression of putative INO80 target genes in control and *INO80* KD morulae. Relative expression of INO80 target genes was determined by qPCR. All data were normalized against endogenous reference gene (*EF1α1*) and control group data were set to 1. C: Expression and localization of OCLN and CHD1 proteins in control and *INO80* KD morulae. Proteins and DNA are represented as green and blue, respectively. Representative images are shown. Experiments were independently repeated three times with at least 15 morulae per group. Scale bar: 100 μm. D: Representative brightfield and fluorescence images of FITC-dextran-treated blastocysts at day 7. Blastocysts from control and *INO80* KD groups were incubated in medium containing 1 mg/mL 40 kDa FITC-dextran for 30 min, then visualized under an inverted fluorescence microscope. Scale bar: 100 μm. E: Analyses of paracellular permeability in trophectoderm by FITC-dextran uptake assay. Number of FITC-positive blastocysts in each group was analyzed. F: Representative brightfield images of chimeric embryos produced by aggregation of C:C, C:K, and K:K embryos at 82 h and 168 h post-activation. Red arrowheads denote blastocysts in C:C and C:K chimeras; blue arrowheads denote aggregates that failed to form blastocysts in K:K chimeras. C: control, K: knockdown. Scale bar: 100 μm. G: Percentage of aggregated or unaggregated embryos. H: Percentage of chimeric embryos that developed to blastocyst or failed to reach blastocyst. Data are mean±*SEM* and different letters on bars indicate significant differences (P<0.05).

al., 2012). Given that *INO80* KD resulted in a reduction in the expression of TJ components, we hypothesized that *INO80* KD may disrupt paracellular sealing of TE cells. Thus, we examined the permeability of the trophectoderm epithelium in porcine blastocysts based on the FITC-dextran (40 kDa) exclusion test. Results showed that the percentage of FITC-positive blastocysts in the *INO80* KD group was significantly higher than that in the control groups (Figure 6D, E), suggesting that the barrier function of the TE epithelium was impaired in *INO80* KD embryos.

To further examine the role of INO80 in TE cells, we conducted an aggregation assay on 8-cell embryos to determine the effects on blastocyst development. The types of aggregation included control-control (C:C) embryos, control-*INO80* KD (C:K) embryos, and *INO80* KD-*INO80* KD (K:K) embryos (Figure 6F). The aggregation rates of the paired embryos were similar among the three groups (Figure 6G). Most C:K paired chimeras overcame the morula-to-blastocyst developmental arrest and developed to the blastocyst stage at a similar rate to the C:C chimeras (Figure 6F, H). In contrast, the K:K paired chimeras could not develop into blastocysts (Figure 6F, H). These results indicate that the control embryos could restore blastocyst development of the *INO80* KD embryos. To determine whether embryo aggregation rescued lineage allocation of the *INO80* KD blastocysts, the C:C and C:K chimera blastocysts were stained with a CDX2 antibody to determine TE cell number (Supplementary Figure S5A). However, no differences were found in the total, TE, and ICM

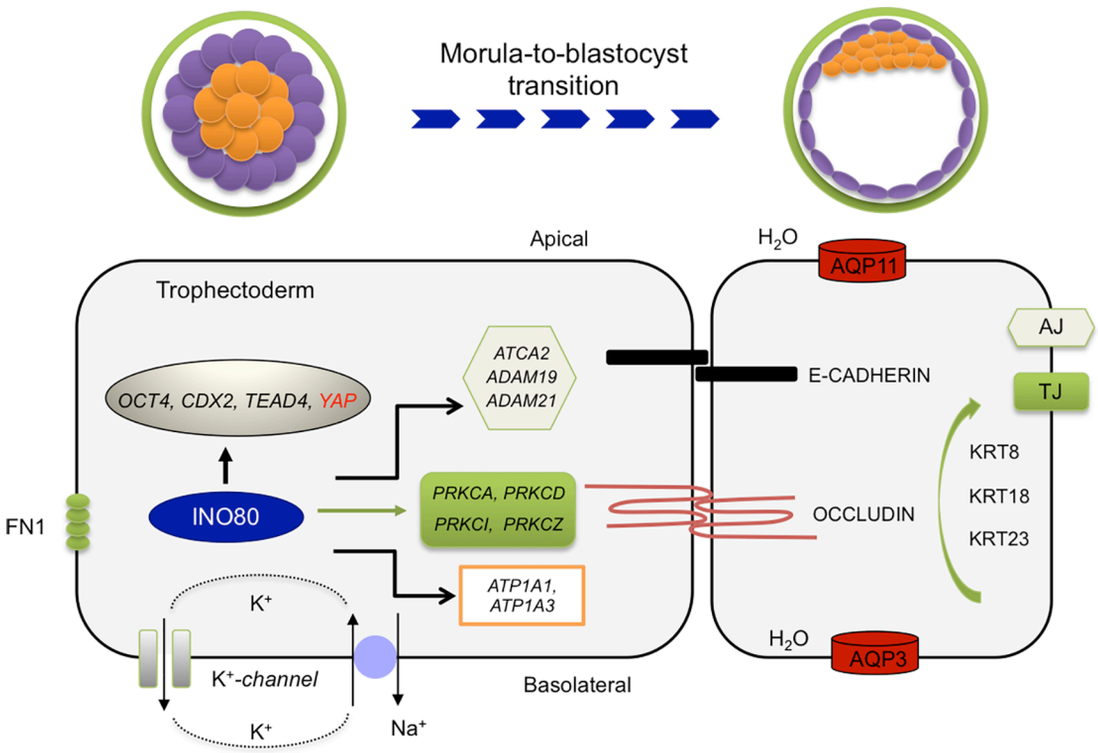

Figure 7 Working model of INO80 modulation of trophectoderm epithelium permeability to promote blastocyst development

In trophectoderm cells, INO80 regulates expression of multiple genes important for lineage specification, tight junction assembly, and fluid accumulation during morula-to-blastocyst transition. Genes shown in black and red are positively and negatively regulated by INO80, respectively. AJ: adherens junction, TJ: tight junction.

cell number or the ICM to TE cell ratio between the C:C and C:K chimeras (Supplementary Figure S5B), indicating restoration of lineage allocation in the *INO80* KD blastocysts. These results demonstrate that INO80 regulates the expression of genes that are essential for the establishment of a functional TE epithelium.

DISCUSSION

Recent studies have reported on the essential role of the chromatin remodeler INO80 in both pluripotency establishment and blastocyst formation in mice (Wang et al., 2014). To date, however, its regulatory mechanism underlying blastocyst development remains poorly known. In the current study, we demonstrated that INO80 promotes blastocyst formation and development in porcine embryos via modulation of the trophectoderm permeability barrier. Mechanistically, INO80 tightly modulates the expression of key genes required for lineage specification, tight junction assembly, and fluid accumulation. Therefore, our data support the model that INO80 regulates blastocyst development by mediating the expression of genes that are essential for lineage specification, tight junction assembly, and fluid accumulation (Figure 7).

Lineage allocation in mammalian blastocysts is mainly regulated by lineage specification-associated transcription factors or transcription co-factors, such as OCT4, CDX2, TEAD4, and YAP (Cao et al., 2019; Nichols et al., 1998; Strumpf et al., 2005; Yagi et al., 2007). Studies have also shown that OCT4, TEAD4, and YAP are essential for blastocyst formation in humans (Fogarty et al., 2017), pigs (Bou et al., 2016; Cao et al., 2019; Emura et al., 2019), and cattle (Daigneault et al., 2018; Negrón-Pérez & Hansen, 2018). CDX2 plays a critical role in blastocyst hatching in pigs (Bou et al., 2017). In this study, we found that *INO80* KD not only blocked porcine blastocyst formation, but also disrupted blastocyst lineage allocation. Moreover, the expression levels of *OCT4*, *CDX2*, and *TEAD4* were down-regulated, whereas that of YAP was up-regulated in the *INO80* KD embryos, suggesting that INO80 is required for their proper expression. Consistent with our findings, a recent mouse study showed that INO80 is implicated in blastocyst formation and expression of pluripotency genes, including *OCT4*, *NANOG*, and *SOX2* (Wang et al., 2014). Thus, our porcine embryo results suggest that INO80 mediates the correct expression of lineage-specification genes to support blastocyst formation and lineage allocation.

Various studies have shown that the epithelial features of TE are an essential prerequisite for blastocoel formation (Choi et al., 2012). Here, single-embryo transcriptome analysis revealed that INO80 is involved in pathways related to the formation of epithelial characteristics. Our results showed down-regulated expression of multiple genes important for TJ assembly (*ADAM19*, *ADAM21*, and *OCLN*), adherens junction formation (*CDH1*), cell polarity (*PRKCD* and *PRKCZ*), and fluid accumulation (*AQP3* and *APQ9*). Although the roles of *ADAM19* and *ADAM21* in blastocyst formation have not been

reported, other isoforms of *ADAM* family genes, such as *ADAM10*, are essential for blastocyst formation in pigs (Kwon et al., 2016), suggesting the potential roles of the *ADAM* family genes in blastocyst development. Earlier research showed that inhibition of the claudin family protein OCLN by neutralizing antibodies can block blastocyst formation in mice (Kim et al., 2004). Adherens junction proteins, such as CDH1, are also required for blastocyst development in mice (Kan et al., 2007). Furthermore, previous studies have demonstrated that the protein kinase C (PKC) family establishes cell polarity networks in epithelial cells and regulates TE formation and blastocyst development in mammals (Eckert et al., 2004; Kalive et al., 2010). Pharmacological inhibition of PRKCD or PRKCZ activity hinders murine blastocyst development (Eckert et al., 2004), and inactivation of PRKCD also prevents bovine blastocyst formation (Yang et al., 2016), indicating that PKC proteins play a conserved role in mice and cattle. Lastly, aquaporin (AQP) proteins have been shown to mediate trans-trophectodermal water transport during blastocoel formation (Barcroft et al., 2003). In mouse embryos, *Aqp3* knockdown blocks blastocyst formation (Xiong et al., 2013). Together, these data indicate that INO80 in porcine embryos facilitates TE development by modulating the expression of key genes involved in TJ assembly and cavitation.

The TJ structure establishes the barrier function of the TE epithelium to support blastocoel formation. In this study, we identified altered expression of key genes involved in TJ assembly. Correspondingly, the permeability of the TE epithelium was also impaired in *INO80* KD embryos. Functional inhibition of *OCLN* in mouse embryos (Kim et al., 2004) and knockdown of *ADAM10* in pig embryos disrupt paracellular sealing (Kwon et al., 2016). This indicates that INO80 mediates TJ assembly to maintain paracellular sealing. Importantly, aggregation experiments in 8-cell embryos revealed that uninjected embryos could complement *INO80* KD embryos and restore blastocyst development and lineage allocation. These results demonstrate that INO80 is a key chromatin remodeler required for TJ assembly and paracellular sealing.

In conclusion, our findings demonstrate that INO80 regulates porcine blastocyst development by mediating the expression of multiple genes required for lineage specification, TJ assembly, and fluid accumulation. Our findings provide new insights into the regulatory mechanisms of chromatin remodeling in porcine blastocyst development.

DATA AVAILABILITY

The sequencing datasets presented in this study can be found in the Gene Expression Omnibus (GEO) online repository of the National Center for Biotechnology Information (NCBI) (accession No.: GSE176436).

SUPPLEMENTARY DATA

Supplementary data to this article can be found online.

COMPETING INTERESTS

The authors declare that they have no competing interests.

AUTHORS' CONTRIBUTIONS

Z.B.C., Y.Y.M., T.Y., Y.S.L., and Y.H.Z. designed the research. D.G., H.L., T.T.X., M.Y.Z., X.W., Q.C.L., Y.L.Y., performed the research. D.G., H.L., and T.T.X. analyzed the data. Z.B.C. and Y.H.Z. wrote the paper. H.Q.Y., Y.Y.M., T.Y., and Y.S.L. revised the manuscript. All authors read and approved the final version of the manuscript.

ACKNOWLEDGMENTS

We thank Dan-Dan Zhang, Meng-Juan Sun, Lu-Yan Shen-Tu, Xiang-Dong Zhang, Zhen-Yuan Ru, and Teng-Long Guo for their technical assistance.

REFERENCES

Alarcon VB. 2010. Cell polarity regulator PARD6B is essential for trophectoderm formation in the preimplantation mouse embryo. *Biology of Reproduction*, **83**(3): 347−358.

Alberio R. 2020. Regulation of cell fate decisions in early mammalian embryos. *Annual Review of Animal Biosciences*, **8**: 377−393.

Barcroft LC, Offenberg H, Thomsen P, Watson AJ. 2003. Aquaporin proteins in murine trophectoderm mediate transepithelial water movements during cavitation. *Developmental Biology*, **256**(2): 342−354.

Bou G, Liu SC, Guo J, Zhao YM, Sun MJ, Xue BH., et al. 2016. Cdx2 represses Oct4 function via inducing its proteasome-dependent degradation in early porcine embryos. *Developmental Biology*, **410**(1): 36−44.

Bou G, Liu SC, Sun MJ, Zhu J, Xue BH, Guo JJ, et al. 2017. CDX2 is essential for cell proliferation and polarity in porcine blastocysts. *Development*, **144**(7): 1296−1306.

Cabot B, Cabot RA. 2018. Chromatin remodeling in mammalian embryos. *Reproduction*, **155**(3): R147−R158.

Cao ZB, Xu TT, Tong X, Wang YQ, Zhang DD, Gao D, et al. 2019. Maternal Yes-associated protein participates in porcine blastocyst development via modulation of trophectoderm epithelium barrier function. *Cells*, **8**(12): 1606.

Chazaud C, Yamanaka Y. 2016. Lineage specification in the mouse preimplantation embryo. *Development*, **143**(7): 1063−1074.

Choi I, Carey TS, Wilson CA, Knott JG. 2012. Transcription factor AP-2γ is a core regulator of tight junction biogenesis and cavity formation during mouse early embryogenesis. *Development*, **139**(24): 4623−4632.

Cockburn K, Rossant J. 2010. Making the blastocyst: lessons from the mouse. *The Journal of Clinical Investigation*, **120**(4): 995−1003.

Daigneault BW, Rajput S, Smith GW, Ross PJ. 2018. Embryonic POU5F1 is required for expanded bovine blastocyst formation. *Scientific Reports*, **8**(1): 7753.

Eckert JJ, McCallum A, Mears A, Rumsby MG, Cameron IT, Fleming TP. 2004. Specific PKC isoforms regulate blastocoel formation during mouse preimplantation development. *Developmental Biology*, **274**(2): 384−401.

Emura N, Takahashi K, Saito Y, Sawai K. 2019. The necessity of TEAD4 for early development and gene expression involved in differentiation in porcine embryos. *Journal of Reproduction and Development*, **65**(4): 361−368.

Fogarty NME, McCarthy A, Snijders KE, Powell BE, Kubikova N, Blakeley P, et al. 2017. Genome editing reveals a role for OCT4 in human embryogenesis. *Nature*, **550**(7674): 67−73.

Goissis MD, Cibelli JB. 2014. Functional characterization of SOX2 in bovine preimplantation embryos. *Biology of Reproduction*, **90**(2): 30.

Hota SK, Bruneau BG. 2016. ATP-dependent chromatin remodeling during

mammalian development. *Development*, **143**(16): 2882−2897.

Kalive M, Faust JJ, Koeneman BA, Capco DG. 2010. Involvement of the PKC family in regulation of early development. *Molecular Reproduction and Development*, **77**(2): 95−104.

Kan NG, Stemmler MP, Junghans D, Kanzler B, de Vries WN, Dominis M, et al. 2007. Gene replacement reveals a specific role for E-cadherin in the formation of a functional trophectoderm. *Development*, **134**(1): 31−41.

Kim J, Gye MC, Kim MK. 2004. Role of occludin, a tight junction protein, in blastocoel formation, and in the paracellular permeability and differentiation of trophectoderm in preimplantation mouse embryos. *Molecules and Cells*, **17**(2): 248−254.

Kwon J, Jeong SM, Choi I, Kim NH. 2016. ADAM10 Is Involved in Cell Junction Assembly in Early Porcine Embryo Development. *PLoS One*, **11**(4): e0152921.

Lee HS, Lee SA, Hur SK, Seo JW, Kwon J. 2014. Stabilization and targeting of INO80 to replication forks by BAP1 during normal DNA synthesis. *Nature Communications*, **5**(1): 5128.

Marikawa Y, Alarcon VB. 2012. Creation of trophectoderm, the first epithelium, in mouse preimplantation development. *In*: Kubiak JZ. Mouse Development: From Oocyte to Stem Cells. Berlin, Heidelberg: Springer, 165–184.

Mordhorst BR, Prather RS. 2017. Pig models of reproduction. *In*: Constantinescu G, Schatten H. Animal Models and Human Reproduction. Hoboken: John Wiley & Sons, 213–234.

Morrison AJ. 2017. Genome maintenance functions of the INO80 chromatin remodeller. *Philosophical Transactions of the Royal Society B: Biological Sciences*, **372**(1731): 20160289.

Negrón-Pérez VM, Hansen PJ. 2018. Role of yes-associated protein 1, angiomotin, and mitogen-activated kinase kinase 1/2 in development of the bovine blastocyst. *Biology of Reproduction*, **98**(2): 170−183.

Nichols J, Zevnik B, Anastassiadis K, Niwa H, Klewe-Nebenius D, Chambers I, et al. 1998. Formation of pluripotent stem cells in the mammalian embryo depends on the POU transcription factor Oct4. *Cell*, **95**(3): 379−391.

Paul S, Knott JG. 2014. Epigenetic control of cell fate in mouse blastocysts: the role of covalent histone modifications and chromatin remodeling. *Molecular Reproduction and Development*, **81**(2): 171−182.

Poli J, Gasser SM, Papamichos-Chronakis M. 2017. The INO80 remodeller in transcription, replication and repair. *Philosophical Transactions of the Royal Society B: Biological Sciences*, **372**(1731): 20160290.

Prather RS, Lorson M, Ross JW, Whyte JJ, Walters E. 2013. Genetically engineered pig models for human diseases. *Annual Review of Animal Biosciences*, **1**: 203−219.

Qiu ZJ, Elsayed Z, Peterkin V, Alkatib S, Bennett D, Landry JW. 2016. Ino80 is essential for proximal-distal axis asymmetry in part by regulating Bmp4 expression. *BMC Biology*, **14**(1): 18.

Serber DW, Runge JS, Menon DU, Magnuson T. 2016. The mouse INO80 chromatin-remodeling complex is an essential meiotic factor for spermatogenesis. *Biology of Reproduction*, **94**(1): 8.

Shan CM, Bao KH, Diedrich J, Chen X, Lu C, Yates III JR, et al. 2020. The INO80 complex regulates epigenetic inheritance of heterochromatin. *Cell Reports*, **33**(13): 108561.

Strumpf D, Mao CA, Yamanaka Y, Ralston A, Chawengsaksophak K, Beck F, et al. 2005. Cdx2 is required for correct cell fate specification and differentiation of trophectoderm in the mouse blastocyst. *Development*, **132**(9): 2093−2102.

Wang HH, Ding TB, Brown N, Yamamoto Y, Prince LS, Reese J, et al. 2008. Zonula occludens-1 (ZO-1) is involved in morula to blastocyst transformation in the mouse. *Developmental Biology*, **318**(1): 112−125.

Wang L, Du Y, Ward JM, Shimbo T, Lackford B, Zheng XF, et al. 2014. INO80 facilitates pluripotency gene activation in embryonic stem cell self-renewal, reprogramming, and blastocyst development. *Cell Stem Cell*, **14**(5): 575−591.

White MD, Plachta N. 2020. Specification of the first mammalian cell lineages in vivo and in vitro. *Cold Spring Harbor Perspectives in Biology*, **12**(4): a035634.

Xiong Y, Tan YJ, Xiong YM, Huang YT, Hu XL, Lu YC, et al. 2013. Expression of aquaporins in human embryos and potential role of AQP3 and AQP7 in preimplantation mouse embryo development. *Cellular Physiology and Biochemistry*, **31**(4–5)): 649−658.

Yagi R, Kohn MJ, Karavanova I, Kaneko KJ, Vullhorst D, DePamphilis ML, et al. 2007. Transcription factor TEAD4 specifies the trophectoderm lineage at the beginning of mammalian development. *Development*, **134**(21): 3827−3836.

Yang QE, Ozawa M, Zhang K, Johnson SE, Ealy AD. 2016. The requirement for protein kinase C delta (PRKCD) during preimplantation bovine embryo development. *Reproduction, Fertility and Development*, **28**(4): 482−490.

Zeng FY, Baldwin DA, Schultz RM. 2004. Transcript profiling during preimplantation mouse development. *Developmental Biology*, **272**(2): 483−496.